Vol. 83 No. 5 pp. 884–892 ACTA GEOLOGICA SINICA (English Edition) Oct. 2009

Petrogenesis of Volcanic Rocks in the Khabr-Marvast Tectonized Ophiolite: Evidence for Subduction Processes in the South-Western Margin of Central Iranian Microcontinent

Azam SOLTANMOHAMMADI[1,*], Mohammad RAHGOSHAY[1] and Morteza KHALATBARI-JAFARI[2]

1 *Faculty of Earth Sciences Shahid Beheshti University, Tehran, Iran*
2 *Institute for Earth Sciences, Geological Survey of Iran, Tehran, Iran*

Abstract: The Late Cretaceous Khabr–Marvast tectonized ophiolite is located in the middle part of the Nain–Baft ophiolite belt, at the south-western edge of the central Iranian microcontinent. Although all the volcanic rocks in the study area indicate subduction-related magmatism (e.g. high LILE (large ion lithophile elements) / HFSE (high field strenght elements) ratios and negative anomalies in Nb and Ta), geological and geochemical data clearly distinguish two distinct groups of volcanic rocks in the tectonized association: (1) group 1 is comprised of hyaloclastic breccias, basaltic pillow lavas, and andesite sheet flows. These rocks represent the Nain–Baft oceanic crust; and (2) group 2 is alkaline lavas from the top section of the ophiolite suite. These lavas show shoshonite affinity, but do not support the propensity of ophiolite.

Key words: alkaline lavas, subduction-related magmatism, tectonized ophiolite, central Iranian microcontinent

1 Introduction

Iranian ophiolites are part of the Tethyan ophiolite belt of the Middle East. These ophiolites link the Middle Eastern ophiolites to other Asian ophiolites. Iranian ophiolites have been divided into two groups: (1) the outer Iranian group of ophiolites, including the Neyriz and the Kermanshah ophiolites, which appear to be coeval with the Oman ophiolite and emplaced onto the Arabian continental margin; and (2) the internal Iranian group of ophiolites that marks the boundaries of the central Iranian microcontinent, including Band-e-ziyarat, Sabzevar, Nain, Shahr-e-babak, Baft, and Tchehel kureh (Fig. 1). In this study, we focus on the geological and geochemical characteristics of volcanic rocks of the Khabr–Marvast tectonized ophiolite in the middle part of Nain–Baft ophiolite belt, which is part of the internal Iranian group of ophiolites.

2 Geology

2.1 Geological setting

The Late Cretaceous Nain–Baft ophiolite belt (as a branch of Neo-Tethys) crops out along the Dehshir Fault. This ophiolite belt extends 350 km in a north-west–south-east direction between the Urumiyeh–Dokhtar magmatic

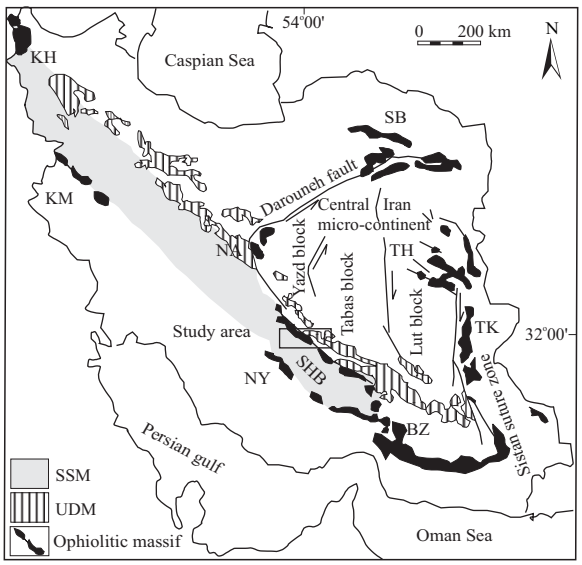

Fig. 1. Description of the ophiolite belts in Iran (based on Emami, et al., 1993) and the location of the study area and its relation to the main tectonic elements of Iran (Ghasemi, 2006). Main Iranian ophiolite complexes: BZ, Band-e-ziyarat; KH, Khoy; KM, Kermanshah; NA, Nain; NY, Neyriz; SB, Sabzevar; SHB, Shahr-e-babak; THL, Torbat Heydariyeh; TK, Tchehel kureh.

* Corresponding author. E-mail: azamsoltanmohammadi@gmail.com

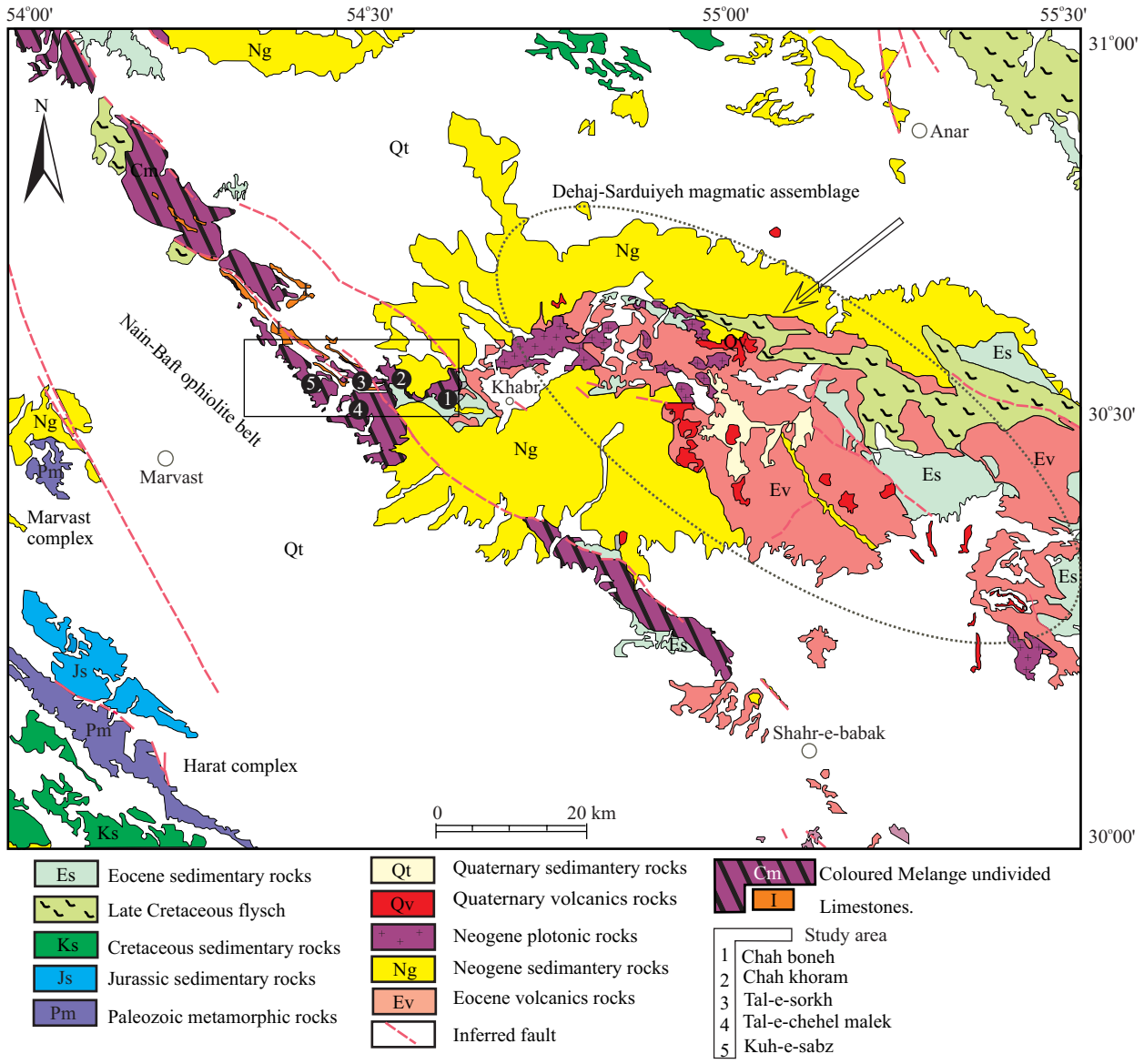

Fig. 2. Schematic geological map of the study area from the Anar quadrangle.

zone (UDM) and the Sanandaj-Sirjan metamorphic zone (SSM). The UDM forms a distinct linear intrusive-extrusive complex with a width of over 4 km (Alavi, 1994).The SSM is a linear metamorphic-magmatic zone in the south-western wedge of the Iranian Plate. In the study area, the Dehaj–Sarduiyeh magmatic assemblage and Marvast–Harat metamorphic complexes are representative of the UDM and SSM, respectively (Fig. 2).

2.2 Ophiolite stratigraphy

The Khabr–Marvast tectonized ophiolite is exposed in the middle part of Nain–Baft ophiolite belt. The field studies in this area led to the recognition of five distinct ophiolite sections, the lithological suites, including from east to west, Chah boneh, Chah khorma, Tal-e-sorkh, Tal-e-chehel malek, and Kuh-e-sabz. These sections represent the oceanic floor, which is made up of various rocks, including pillow lavas, sheet flows, sheeted-dike complexes, isolated dikes belonging to the crustal section, and peridotites, from the mantle section.

The mantle section peridotites are frequently exposed in the area and generally show the evidences for sea-floor metasomatism. This ultramafic unit is composed of serpentinized harzburgite with minor dunite lenses. Further up section, mesocratic isotropic gabbros dominate. These mafic rocks range from olivine gabbro to micro gabbro; diabase rarely contain paths of pegmatoidal phases. Still upward in the crustal section, sheeted-dike complexes appear in the section of Chah boneh and Tal-e-chehel malek. These dikes have variable mineral assemblages varying in lithology from diabase to lesser quartz diabase and gabbro. Extrusive sequence are dominated by hyaloclastic breccias as small blocks within the sheeted-dike complexes from the Chah boneh area. At

Tal-e- chehel malek, this sequence is represented by massive lavas turning into pillow basalts to the top of the section, which vary in size from small to large bodies. A characteristic of the bodies is the occurrence of amygdales composed of minerals, such as calcite, quartz, and chlorite. Also, well-exposed andesite sheet flows, interlayered with radiolarite beds, occur in the Tele-sorkh section covered totally by the latter to the top of this section. These ophiolitic rocks are cut by numerous isolated dikes, which range from pegmatite gabbro, diabase, to quartz diabase.

Laterally, in the top section of the ophiolite suite, some volcanic rocks exist. These rocks occur as dikes and massive bodies, represented in the Tal-e-chehel malek section by numerous basaltic dikes cross-cutting, massive and pillow basalts that are approximately 1 m in thickness, and by massive olivine basalts to the top sections of the ophiolite suite, which locally cover he peridotites in the north of Chah boneh. Stratigraphically, these volcanic rocks are inferred to be younger in age than the underlying, ophiolite suite.

3 Petrography

Andesite sheet flows, basaltic pillow lavas, and hyaloclastic breccias have been subjected to various degrees of ocean-floor hydrothermal alterations. This implies the transformation of clinopyroxene into termolite–actinolite or chlorite, whereas plagioclase is replaced by albite, epidote, prehnite, and kaolinite. Most of the basaltic pillow lavas display a wide range of textures, ranging from fine-grained aphyric to intersertal and intergranular. In some samples, plagioclases can be found as phenocrysts and also as matrix minerals displaying characteristic “bow-tied” and “swallow-tailed” quench forms. Clinopyroxene with a xenomorphic shape are another indication of the quench nature of these rocks (Shelley, 1993) (Fig. 4B–4D). All of these forms of minerals indicate sub-marine volcanism (Juteau, 1999). In addition, amygdaloidal and glomeroporphyritic textures are found. Andesite sheet flows show consistently porphyritic textures within these samples with altered phenocrysts of plagioclase and clinopyroxene.

The majority of studied lavas in the top section of the ophiolite suite are seriate-textured rocks dominated by unaltered clinopyroxenes and plagioclases. Phenocrysts of oscillatory-zoned plagioclases, sometimes have sieve texture or dusty zones (Fig. 4F). In addition, olivine basalts from thin sections show iddingsitized olivines. In all of the lithologies, opaques constitute the main accessory minerals that occur within similar ground masses.

4 Geochemistry

4.1 Classification of rocks

Selective whole-rock analyses for the samples studied in this paper are given in Table 1. Geochemical studies further support our earlier hypothesis, which is based on field studies and petrographic observations. The existence of two different groups of lavas probably originated from magma with contrasting compositions. These include: (1) ophiolitic lavas, which are composed of hyaloclastic breccia, basaltic pillow lavas, and andesite sheet flow, and are genetically related to the plutonic part of ophiolites (not shown); and (2) alkaline lavas, which can be found in the top sections of the ophiolite suite as dike or massive bodies.

Many diagrams conventionally used to classify igneous rocks utilize mobile elements, which commonly renders them unreliable for classifying rocks from the geological record (e.g. the K_2O–SiO_2 diagram) (Hastie, et al., 2007). By using Th as a proxy for K_2O and Co as a proxy for SiO_2, it is possible to construct a topologically-similar diagram that performs the same task, but is more robust for hydrothermally-altered volcanic arcs. Thus, because of the altered nature of volcanic rocks in this study, the same approach has been followed for the classification of these rocks (Fig. 3). As shown in Fig. 3, the composition of pillow lavas and sheet flow extend the fields represented by the tholeiitic basalt and calc-alkaline andesite, and for olivine basalts and basaltic dikes, by high K-shoshonitic and andesite basalts.

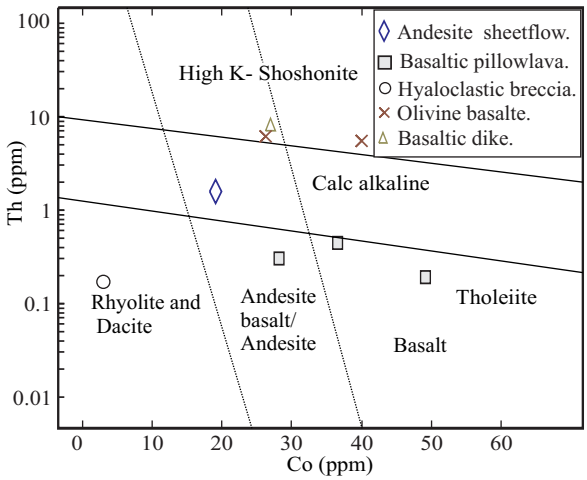

Fig. 3. Plot of the volcanic samples in this study in the Th–Co discrimination diagram (Hastie, et al., 2007) showing varying affinities from tholeiite to high K- shoshonite .

4.2 Trace elements

The primitive, mantle-normalized multielement plot

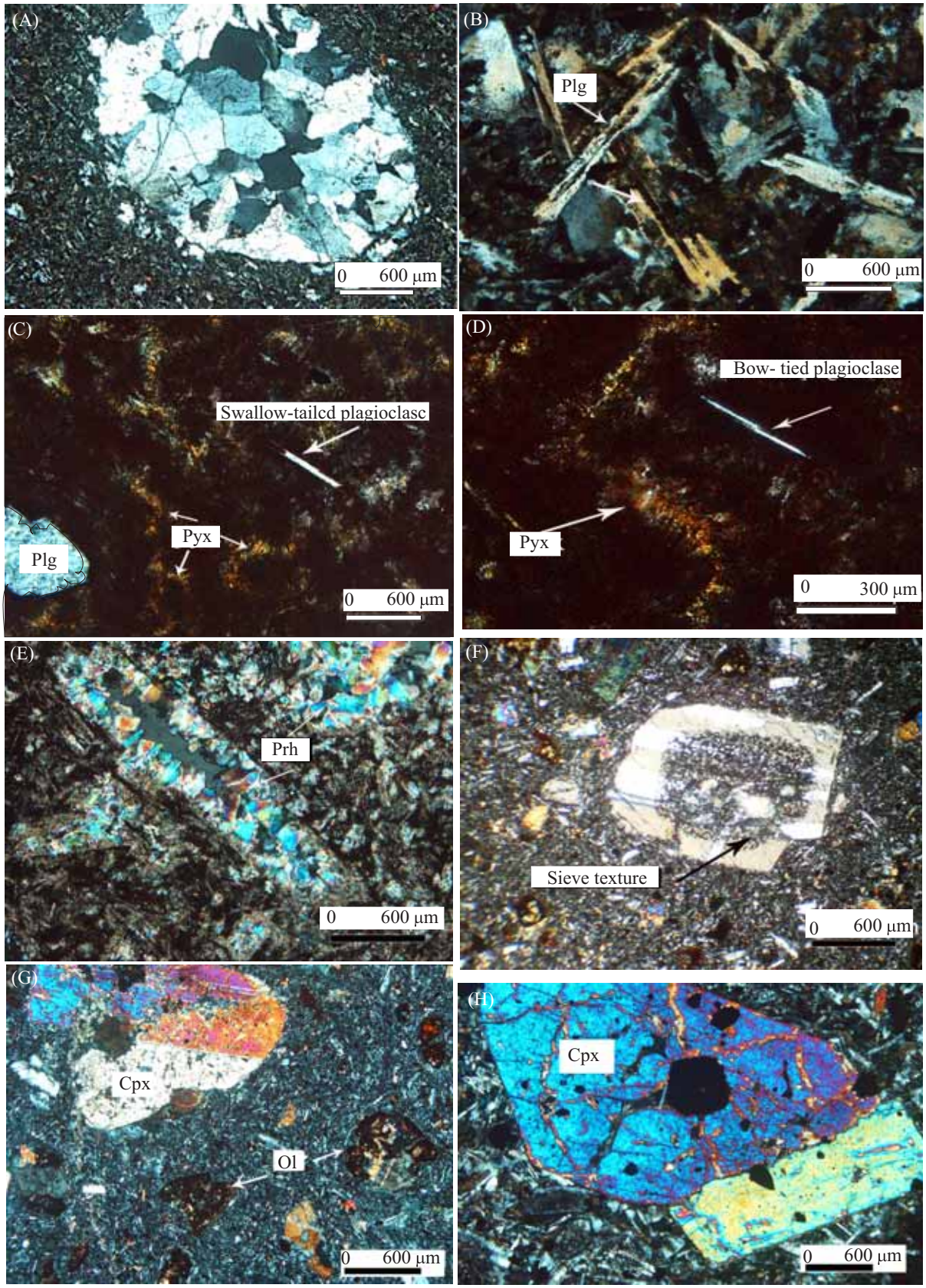

Fig. 4. Microphotograph of volcanic rocks in the study area. (A) Amygdale filled with quartz in altered basalt; (B, C, D) examples of quenched plagioclases (PLG) and pyroxenes (PYX) in basalt: "swallow-tailed" and "bow-tied" microlites; (E) pseudomorphous phenocrysts in andesite sheet flow replaced by columnar prehnite; (F) development of sieve texture in plagioclase phenocrysts in olivine (OL) basalt; (G) iddingsitized olivines and fresh clinopyroxene phenocrysts (CXP) in olivine basalt; (H), large, euhedral phenocrysts of clinopyroxene with euhedral, opaque inclusions in porphyritic basalt.

Table 1 Whole-rock analyses of selected samples

Sample	Ophiolitic lavas					Alkaline lavas		
	Pil.B	Pil.B	Pil.B	An.Sh	Hy.B	Ol.B	Ol.B	B.Di
SiO_2	54.7	48.8	56.1	56.5	72.7	54	49.9	49.2
TiO_2	1.42	1.2	2.37	1.03	0.03	0.81	0.85	0.72
Al_2O_3	14.15	14.7	11.1	14.65	11.2	17.5	17.7	15.5
Fe_2O_3	11.75	11.1	14.3	8.85	4.91	8.62	10	10.4
MnO	0.2	0.19	0.24	0.12	0.07	0.14	0.17	0.23
MgO	3.52	7.96	3.62	1.48	1.56	4.22	5.89	3.5
CaO	8.2	11.3	6.1	3.7	1.72	7.55	9.44	8.66
Na_2O	3.88	2.05	4.3	7.5	4.29	3.24	2.8	2.52
K_2O	0.07	0.09	0.07	0.07	0.1	2.82	1.57	3.51
P_2O_5	0.16	0.06	0.15	0.3	0.03	0.31	0.26	0.6
Total	99.8	99.9	99.7	98.2	99.3	101.10	99.63	98.6
Ba	61.3	87.1	95.2	70.6	29.4	595	261	913
Rb	1.2	1.3	1.3	1.3	0.8	112	57.4	107.5
Sr	83.9	154.5	59.9	51.2	71.1	491	598	1040
Y	28.1	23.5	40.2	24.6	36.3	24.4	21.4	25.7
Zr	66	59	128	82	69	108	85.6	131
Nb	1.1	1.3	3.4	2.1	1	4.34	3.43	6.4
Ta	0.098	0.099	0.2	0.1	0.098	0.299	0.23	0.3
Th	0.3	0.19	0.44	1.61	0.17	5.4	4.11	8.31
Pb	42	201	246	114	5	13.9	7.19	1280
Zn	190	182	292	92	69	79	76	1420
Cu	86	61	45	30	7	70	110	231
Ni	12	104	20	10	5	19	36	10
V	387	352	527	303	5	240	301	246
Cr	50	340	100	20	10	22.3	59.6	40
Co	28.1	49.1	36.5	19.1	3	24.2	38.8	26.9
U	0.26	0.12	0.51	0.53	0.13	1.87	1.34	2.59
Ti	8511.466	7192.788	14205.76	6173.81	1798.197	4856.93	5147.639	4315.673
La	3.1	2.6	6.3	8	1.3	17.6	16.4	30.2
Ce	9.2	7.8	17.1	19.3	5.6	35.7	33.5	59.6
Pr	1.53	1.28	2.72	2.73	1.05	4.53	4.46	7.29
Nd	8.3	6.6	13.8	12.5	6.1	18.9	18.2	29.1
Sm	2.85	2.32	4.43	3.42	2.68	4.44	4.02	6.33
Eu	1.23	0.92	1.46	1.16	0.96	1.26	1.18	1.86
Gd	3.76	3.05	5.49	3.82	3.82	3.91	3.42	6.32
Tb	0.74	0.6	1.02	0.69	0.8	0.651	0.577	0.91
Dy	4.98	4.11	6.96	4.41	6	3.99	3.67	4.88
Ho	1.04	0.91	1.53	0.98	1.38	0.868	0.741	1
Er	3.18	2.69	4.53	2.77	4.24	2.22	1.86	2.82
Tm	0.47	0.38	0.67	0.41	0.65	0.357	0.326	0.38
Yb	3.13	2.51	4.37	2.68	4.39	2.38	1.82	2.54
U	0.48	0.38	0.65	0.42	0.7	0.35	0.298	0.41
Th/Ta	3.06	1.91	2.2	16.1	1.73	18.06	17.86	27.7
Ba/Th	204.33	458.4211	216.3636	43.580	172.941	110.185	63.50	109.867
Th/Ce	0.032	0.024	0.025	0.083	0.030	0.15	0.12	0.13
$La_{(n)}/Yb_{(n)}$	0.71	0.74	1.03	2.14	0.21	5.32	6.46	8.52

An.Sh, andesite sheet flow; B.Di, basaltic dike; Hy.B, hyaloclastic breccias; Ol.B, olivine basalt; Pil.B, pillow basalt.

(Sun and McDonough, 1989) for hyaloclastic breccia, pillow basalts, and andesite sheet flow are presented in Fig. 5. As shown in Fig. 5, these rocks are enriched in Ba, U, and Pb and depleted in HFSE (Nb and Ta) (Fig.5). However, chondrite-normalized rare earth element (REE) plots for these samples in Fig. 5 show slightly depleted–slightly enriched light REE (LREE) with respect to heavy REE (HREE). On the basis of trace element content of the rocks, three lava subgroups have been defined: (1) hyaloclastic breccia characterized by a slight depletion in LREE, as compared to that of N-type mid-ocean ridge basalts (N-MORB) (Fig. 6A); (2) basaltic pillow lavas show flat REE spectra in chondrite-normalized plots, similar to those of N-MORB, but with an elevated LREE content ($La_{(n)}/Yb_{(n)}$~0.7–1.08); and (3) andesite sheet flow with a higher LREE concentration compared to other subgroups (30~40×chondrite) ($La_{(n)}/Yb_{(n)}$~ 2.14) similar to that of E-type mid-ocean ridge basalts.

These variable patterns are common in the supra-subduction-type ophiolites, which might reflect the presence of a heterogeneous source for the generation of these rocks.

In contrast, the second group in the chemical classification (alkaline lavas) has a higher K_2O (1.5%–3.5% weight) rather than ophiolitic lavas. Trace element patterns of these lavas show strong LILE, Th, and LREE enrichments (Fig. 5). In addition, these lavas show negative HFSE (Nb, Ta, Ti, Zr, and Hf) anomalies relative

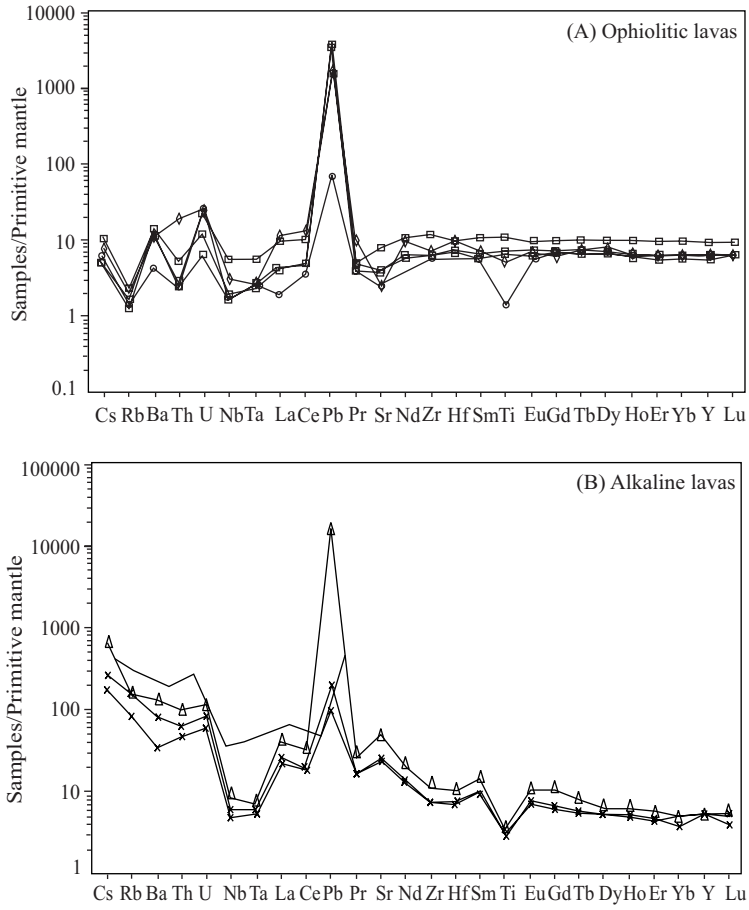

Fig. 5. Primitive mantle-normalized incompatible trace element diagram for (A) ophiolitic and (B) alkaline lavas in this study.
Normalizing data are from Sun and McDonough (1989).

to LILE and Ce, which are also higher for the respected values for these elements in the mantle. The chondrite-normalized REE plots of these alkaline lavas show typical Oceanic island basalt(OIB)-like geochemical characteristics (Fig. 6B). However, they show negative anomalies in Nb, Ta, and Ti in contrast with the geochemical features of OIB (Hawkesworth et al., 1991).

5 Tectonic Setting and Petrogenesis

Fig. 7 shows the widely- used tectonomagmatic-discriminant diagram of Wood (1979) that employs the elements Th, Ta, and Hf. This diagram displays the island arc tholeiite (IAT) nature of ophiolitic lavas, except for the sample from the andesite sheet flow. In contrast, the alkaline samples display significant Th enrichment and plot in the calc-alkaline basalts in the subduction zone setting (Fig. 7).

Th/Yb versus Ta/Yb is used to differentiate between depleted mantle (MORB) and enriched mantle (intraplate) sources (Pearce, 1982) (Fig. 8). For subduction-related magmatic rocks, the addition of a subduction chemical component by slab-derived fluids/ melting results in an increase of Th/Yb in the mantle source. The data from selected samples are consistent with the derivation of a MORB-type depleted mantle source enriched by subduction zone components. The alkaline lavas differ from the others by having high Ta and Th contents, which suggests their derivation from an enriched source (Fig. 8). Pearce et al (2005) used elements, such as Ba, Th, and Nb, to identify the subduction component in the lavas of the Mariana arc–basin system. These elements are all highly incompatible and behave in a similar manner during melting and fractional crystallization. However, they are decoupled by subduction processes. Ba and Th are significantly partitioned into siliceous melts, but only Ba is also extensively partitioned into aqueous fluids derived from the subducted slab. Nb is possibly mobilized only in deep melts at the highest temperatures or by very

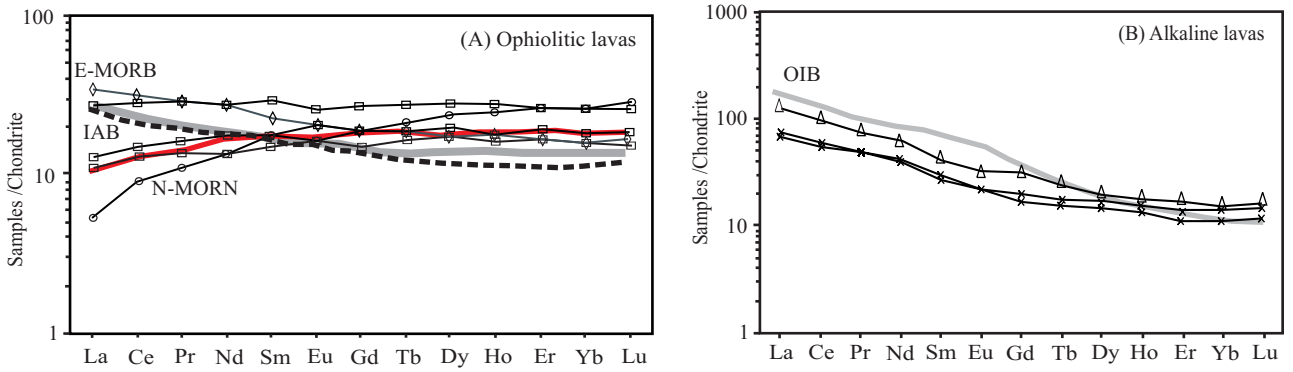

Fig. 6. Chondrite-normalized rare earth element patterns of (A) ophiolitic and (B) alkaline lavas. Normalizing values based on Sun and McDonough (1989).
Average composition of oceanic island basalts (OIB). N-type and E-type mid-ocean ridge basalts (N-MORB and E-MORB, respectively) are from Sun and McDonough (1989) and McDonough and Sun (1995), and the average composition of island arc basalts (IAB) is from Elliott (2003).

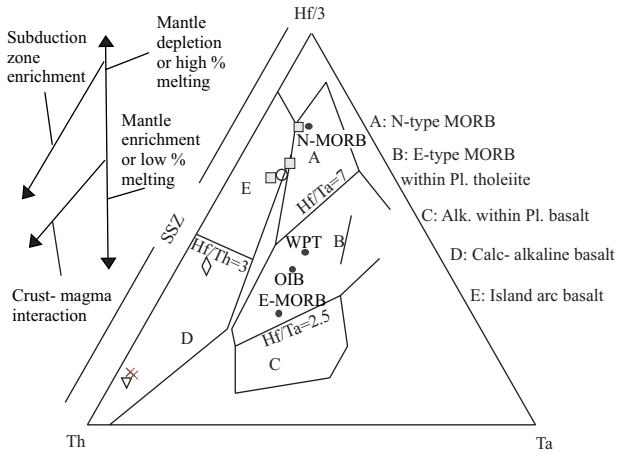

Fig. 7. Hf/3–Th–Ta tectonomagmatic-discriminant diagram (Wood, 1979).

Values for N-type mid-ocean ridge basalts (N-MORB), oceanic island basalts (OIB), and E-type mid-ocean ridge basalts (E-MORB) are based on Sun and McDonough (1989).Trend of vectors are from Koglin (2008). SSZ; Suprasubduction zone

low degrees of melting. Ratios in the studied samples show that the lavas are influenced by different subduction-related components. Ophiolitic lavas have higher Ba/Th (172–485) and lower Th/Ta (1.7–3.06) ratios. These amounts indicate that fluids derived by dehydrating subducted materials play a main role in the generation of these rocks (e.g. Munker, et al., 2004; Pearce, et al., 2005).

The low Th/Ce ratio suggests that crustal contamination does not play a significant role in the generation of magma because the continental crust has relatively high Th/Ce ratios (~0.15) (Taylor and McLennan, 1995), whereas mantle-derived magma have low Th/Ce ratios (0.02–0.5) (Sun & Stern, 2001). Ophiolitic lavas with low Th/Ce

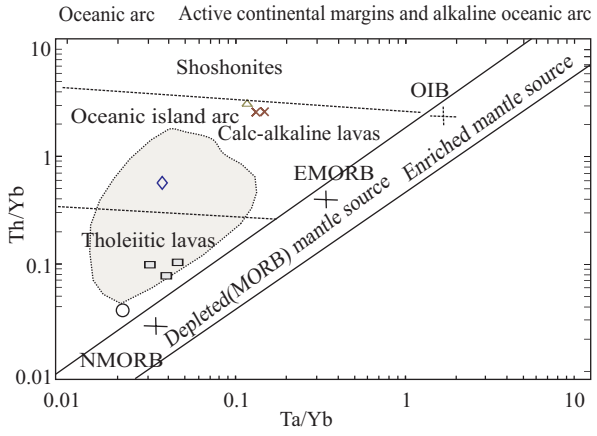

Fig. 8. Th/Yb–Ta/Yb ratio plot of Pearce (1982), which provides an immobile element method of identifying arc lavas and their volcanic series.

E-MORB, E-type mid-ocean ridge basalts; N-MORB, N-type mid-ocean ridge basalts; OIB, oceanic island basalts.

(0.02–0.04) ratios are similar to the Lau Basin and Mariana as the oceanic basin (not shown), whereas alkaline lavas have higher Th/Ce ratios (0.12–0.15), which indicates that the addition of slab-derived components and or crustal contamination might play a role in the generation of magma; however, this characteristic is compared to an enriched source. The concentration of trace elements indicates that strong fraction of LREE relative to HREE in the alkaline lavas could be due to the involvement of certain refractory phases (e.g. garnet). However, melting with residual garnet should exhibit not only greater LREE enrichment, but also steeper HREE patterns. Model calculations by Lin et al (1989) predicted REE evolution in spinel peridotite melts. Melt generated from a spinel peridotite after different extents of melting have variable LREE enrichment, but rather flat HREE patterns (e.g. studied samples in this paper).

Fig. 9 provides a proposed tectonic discrimination between shoshonites from oceanic and continental settings (Hawkesworth, et al., 1991). Those from oceanic island arcs have Ce/Yb ratios less than about 45, whereas shoshonites from post-collisional or continental arc settings mostly have ratios exceeding 45 (Sun and Stern, 2001). The distinction may in parts reflect the control imposed by the thickness of the cool lithosphere on the proportion of melting that occurs in garnet and/or spinel peridotite facies. Aeolian potassic rocks, which erupted in an arc formed on a thinned continental crust and lithosphere, fall in the oceanic domain in Fig. 9. The lithospheric thinning has allowed the upwelling of the wedge asthenosphere to relatively shallow depth, where a greater proportion of spinel facies melting can contribute to magma generation. The alkaline lavas in this paper fall in the oceanic domain (Fig. 9), and flat patterns in HREE for these lavas indicate the occurrence of melting in spinel peridotite facies. These characteristics indicate that garnet might have a role in the generation of alkaline lavas (because of higher Ce/Yb ratios), but probably it had not been of significant contribution .

6 Discussion and Conclusion

Although ophiolitic complexes of Iran are part of the eastern Mediterranean ophiolites and known as supra-subduction-type ophiolites, the petrogenesis and tectonic setting of volcanic rocks in the so-called “Shahr-e-babak ophiolites” still remain ambiguous (e.g. island arc setting; Ghazi & Hassanipak, 2000, back-arc basin; Shafaii et al., 2008; Shahabpour, 2005)..The geological and geochemical data presented here on volcanic rocks of Khabr–Marvast tectonized ophiolite (northwest of “Shahr-e-babak ophiolites”) indicate the existence of two distinct volcanic

associations, namely the ophiolitic lavas and alkaline lavas. The first group includes the hyaloclastic breccias, basaltic pillow lavas, and andesite sheet flows, the petrographic and geochemical characteristics of which indicate parts of an oceanic crust. The concentration of trace elements in these lavas reflect melting in the stability field of spinel peridotite with the variable enrichment of LREE with respect to flat HREE. High Ba/Th and low Th/Ta ratios point to hydrous melting in a supra-subduction zone environment.

Alkaline lavas, including olivine basalt and basaltic dikes in the top section of the ophiolite suite, have shoshonite affinity. The HFSE depletions in these lavas indicate genesis in a subduction-zone setting. This characteristic is unlikely to be resulted from melting any oceanic island basalt (OIB) mantle source as advocated before for these kinds of rocks. Although alkaline lavas show elevated concentrations of LILE, but fluid-sensitive element ratios (e.g., Ba/Th) for these lavas are lower than the ratio for ophiolitic lavas, we conclude that the enriched compositions of the shoshonitic series did not result from the melting mantle that was metasomatized by hydrous fluids. Th and other incompatible elements together may reflect slab-derived components obtained without fluid mediation.

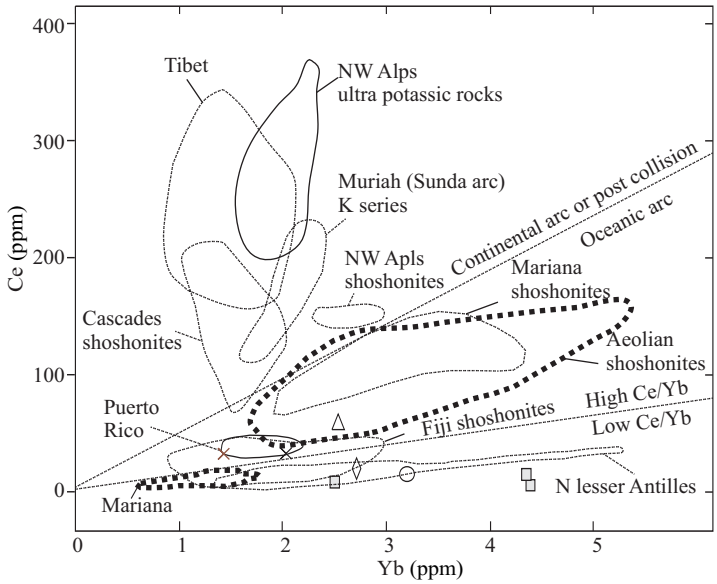

Fig. 9. Ce versus Yb in the studied samples and in various shoshonite and potassic associations in other parts of the world.
(—) Shoshonite data from post-collisional settings; (-.-.-.) continental arc compositions, (---) oceanic arc data. Diagram adapted from Sun and Stern (2001). Tibet data are from Turner et al (1996); cascade absarokite/shoshonite data are from Leeman et al (1990), Corney et al (1997), and Bacon (1990). Continental/oceanic dividing line lie at a Ce/Yb ratio of 46.5; high/low Ce/Yb boundary line is from Hawkesworth et al (1991).

We have no solid evidence for the ophiolitic nature of the alkaline lavas. According to field studies, these lavas are younger than the basal ophiolite suite. Thin-section observations of the lavas have shown that ophiolitic lavas, apart from the alkaline lavas, have been affected by oceanic low-temperature hydrothermal alteration events. The geochemical characteristics indicate different magma for the generation of alkaline lavas (enriched source). Finally, we propose the term “post-ophiolite” for alkaline lavas, which is consistent with the model that assumes the subduction of the Arabian plate under the central Iran microcontinent.

Acknowledgements

We would like to acknowledge the helps by all of those who in any way contributed to this work. Our special thanks are due to Dr. M. A. Mackizadeh (Univ. of Isfahan) and A. Esmaeeli (Damghan Univ.) who assisted during the fieldwork. Sarem Amini (Univ. of Shahid Beheshti) reviewed and improved the English manuscript. Finally, We appreciate the efforts by an anonymous editor who corrected the initial manuscript and greatly improved it.

Manuscript received Aug. 22, 2009
accepted Sept. 15, 2009
edited by Fei Hongcai

References

Alavi, M., 1994. Tectonics of the zagros orogenic belt of Iran: new data and interpretations. *Tectonophysics*, 229: 211–238.

Bacon, C.R., 1990. Calc-alkaline, shoshonitic, and primitive tholeiitic lavas from monogenetic volcanoes near Crater Lake, Oregon, *J.Petrol*., 31: 135–166.

Conrey, R.M., Sherrod, D.R., Hooper, P.R., and Swanson, D.A., 1997. Diverse primitive magmas in the Cascade arc, northern Oregon and southern Washington, *Can. Mineral*., 35: 367– 396.

Elliott, T., 2003. Tracers of the slab, *Geophysical Monograph*, 238: 23–45.

Emami, M.H., Sadegi, M.M., and Omrani, S.J., 1993. Magmatic map of Iran. Scale 1:1 00 000, *Geological Survey of Iran*.

Ghasemi, A., and Talbot, C.J., 2006. A new tectonic scenario for the Sanandaj-Sirjan zone (Iran). *Asian*

Earth sci. J., 26: 683–693.

Ghazi, A.M., and Hassanipak, A.A., 2000. Petrology and geochemistry of the Shahr-babak ophiolite, cenral Iran. In: Dilek, Y., Moores, E.M., Elton, D., and Nicolas, A. (eds.), Ophiolites and oceanic crust: New insight from field studies and the ocean drilling program: Boulder, Colorado. *Geo. Soc. Spec.Pap*, 349: 485–497.

Hastie, A.R., Keer, A.C., Pearce, J.A., and Mitchell, S.F., 2007. Classification of altered volcanic island arc rocks using immobile trace elements: development of the Th-Co discrimination*, J*., *Petrology.* 48 (12): 2341–2357.

Hawkesworth, C.J., Hergt, J.M., Ellam, R.M., and MacDermott, F., 1991. Element fluxes associated with subduction related Magmatism, Philos. Trans. R. Soc. Lond. Ser. *A: Math Phys Sci*, 335: 393–405.

Juteau, T., and Maury, R., 1999. The oceanic crust, from accretion to mantle recycling , springer-praxis, chichester, UK, ch7.

Koglin, M., Kostopoulos, and D., Reischmann, T., 2008. The lesvos mafic-ultramafic complex, Greece: ophiolite or incipient rift?, *lithos,* doi:10.1016/ j.lithos.2008.09.006

Leeman, W.P., Smith, D.R., Hildreth, W., Palacz, Z., and Rogers, N., 1990. Compositional diversity of late Cenozoic basalts in a transect across the southern Washington Cascades: implications for subduction zone magmatism, *Geophys. Res. J*., [Solid Earth] 95: 19561–19582.

Lin, P.N., Stern, R.J., Morris, J., and Bloomer, S.H., 1989, Shoshonite volcanism in the northern Mariana Arc: Evidence for the source of incompatible element enrichment in intraoceanic arcs*, Geophys Res. J*., 94: 497–4514.

McDonough, W.F., and Sun, S.S., 1995.The composition of the Earth, *Chemical Geology*, 120: 223–253.

Münker, C., Wörner, G., Yogodzinski, G., and Churikova, T., 2004. Behaviour of high fieldstrength elements in subduction zones: constraints from arc lavas rocks in the Kamchatka–Aleutian region, *Earth Planet Sci Lett*, vol. 224: 275–293.

Pearce, J.A., 1982. Trace element characteristics of lavas from destructive plate Boundaries, In: Thorpe, R.S. (Ed.), Andesites: Orogenic Andesites and Related Rocks. *John Wiley and Sons*: 252–548.

Pearce J.A., Peate, D.W., 1995. Tectonic implications of the composition of volcanic arc magmas. *Annu. Rev. Earth Planet. Sci*, 23: 251– 285.

Pearce, J.A., Stern, R.J., Bloomer, S.H., and Fryer, P., 2005, Geochemical mapping of the Mariana arc-basin system: implications for the nature and distribution of subduction components, *Geochemistry, Geophysics, Geosystems*, 6, Q07006 doi:10.1029/ 2004GC000895.

Shafaii Moghadam, H., Rahgoshay, M., and Whitechurch, H., 2008. The Mesozoic back-arc extension in the active margin of Iranian continental block: constrain from age and the geochemistry of the mafic lavas*, Ofioliti*., 23(2): 95–103.

Shahabpour, J., 2005. Tectonic evolution of the orogenic belt in the region located between Kerman and Neyriz, *Asian Earth sci. J*., 24: 652–665.

Shelley, D., 1993. *Igneous and metamorphic rocks under the microscope*. Chapman and Hall, London, UK. 175–178.

Sun, S.S., and McDonough, J.D., 1989. Chemical and isotopic systematics of oceanic basalts: implications for mantle composition and process, in: Magmatism in the Ocean Basins*, Geol. Soc. Spec. Pap*, 42: 313–345.

Sun, C.H., and Stern, R.J., 2001. Genesis of Mariana shoshonites: contribution of the subduction component, *Geophys. Res. J.,* [Solid Earth] 106: 589–608.

Taylor, S.R. McLennan, S., 1995. The geochemical composition of the continental crust, *Rev. Geophys*, 33: 241–265.

Taylor, R.N., Nesbitt, R.W., 1988. Light rare-earth enrichment of supra-subduction zone mantle: evidence from the Troodos ophiolite, Cyprus*. J*., *Geology.* 16: 448–451.

Turner, S., Arnaud, N., Liu J., Rogers, N., Hawkesworth, C., Harris, N., Kelley, S., van Calsteren, P., and Deng, W., 1996. Postcollision, shoshonitic volcanism on the Tibetan Plateau: implications for convective thinning of the lithosphere and the source of ocean island basalts*, Petrol. J*., 37: 45– 71.

Wood, D.A., Joron, J.L., and Treuil, M., 1979, A re-appraisal of the use of trace elements to classify and discriminate between magma series erupted in different tectonic settings: *Earth and Planetary Science Letters*, 45: 326–336.